

# 行政院國家科學委員會專題研究計畫 成果報告

## 多電子束平行掃瞄微影系統設計--子計畫三：多電子束平行掃瞄系統之電磁透鏡、遮黑板與資料傳輸系統研發(I) 研究成果報告(精簡版)

計畫類別：整合型  
計畫編號：NSC 95-2221-E-002-308-  
執行期間：95年08月01日至96年07月31日  
執行單位：國立臺灣大學電機工程學系暨研究所

計畫主持人：蔡坤諭  
共同主持人：盧奕璋、李佳翰  
計畫參與人員：參與人員：劉俊宏、謝良軒、陳信全、陳信宏

處理方式：本計畫可公開查詢

中華民國 96年10月25日



# 多電子束平行掃瞄微影系統設計-子計畫三：多電子束平行掃瞄系統之電磁透鏡、遮黑板與資料傳輸系統研發 (I)

## Development of Electro-magnetic Lens, Blanker, and Data Transmission Systems for E-beam Based Massively Parallel Maskless Lithography (MPML2) Systems

計畫編號：NSC95-2221-E-002-308

執行期限：95年8月1日至96年7月31日

主持人：蔡坤諭教授 國立台灣大學電機工程學系暨研究所

計畫參與人員：劉俊宏、謝良軒、陳信全、陳信宏 國立台灣大學電機工程學系暨研究所

### Abstract

Massively parallel maskless lithography (MPML2) system has been developed by the joint group in National Taiwan University. MPML2 is a multiple electron beam direct-write system which aims at 22 nm node semiconductor manufacturing. For electrostatic lens design of MPML2, a simulator capable of 2D and 3D electrostatic lens simulation is implemented. This simulator consists three parts: field computation, trajectory simulation, and optical performance evaluation. Electrostatic field of lenses is evaluated via finite element method (FEM) with the core of COMSOL Multiphysics, while the other two parts are developed under MATLAB environment. For electron trajectory simulation, ideal and practical trajectories can be computed. For optical property evaluation, the primary geometrical and chromatic aberrations are evaluated for rotationally symmetrical lenses. Besides the conventional aberration analysis, direct ray tracing method for minimum spot size is also proposed and implemented. Finally, this simulator is applied to e-beam direct-write system design and analysis for preliminary lens design of MPML2. The Lens parameters of MPML2 are determined successfully.

Keywords —e-beam; maskless; electrostatic; electron optics; lithography

### 中文摘要

多電子束平行無光罩微影系統(MPML2)已由台灣大學研究團隊所開發。MPML2是一個目標在半導體製造裡可以寫出22奈米線寬的多電子束直寫式系統。對於MPML2裡的靜電透鏡設計來說，開發出一適用二維與三維靜電透鏡模擬與分析之環境。此模擬環境包含三個部份：靜電場的計算，電子軌跡的模擬，以及光學特性的評估。靜電透鏡內的電場大小可藉由COMSOL Multiphysics內的有限元素法去分析，而另外兩部份的開發則是在MATLAB環境下操作。以電子束軌跡的模擬來看，理想與實際的電子束軌跡則可被計算出。對於光學特性的評估，主要的幾何像差與色散像差則是在旋轉對稱式透鏡內去分析。此外，一般像差分析的方法裡，適用於最小聚焦點分析的直接追蹤軌跡方法則是被提出來並應用。最後，此模擬環境適用於其MPML2初代靜電透鏡系統之設計與分析上。另外MPML2初代透鏡內的參數則很成功的被評估出來。

關鍵字：電子束；無光罩；靜電；電子光學；微影

## 1. Introduction

It is known that optical lithography with 193 nm ultraviolet faces the physical limitation in 22 nm node integrated circuit (IC) fabrications. Though extreme ultraviolet (EUV) lithography is capable of the resolution under 22 nm, some technological and financial problems still obstruct its way. Electron beam lithography is one of the promising technologies for 22 nm node IC fabrications [1][2]. For the purpose of improving system throughput, array of e-beams should be driven at one time, and large amount of miniature electron optical elements are required. Electrostatic type electron optical elements are preferred for multiple e-beam lithography systems, since their physical structures are simple compared to magnetic type [3].

Lens governs the imaging properties of the electron optical systems (EOS), while simulation tools for EOS design or analysis are rare and expensive. In the first part of this article, a simulator capable of 2D and 3D electrostatic lens simulation is implemented for the application to the next generation e-beam direct-write system design. This simulator consists three parts: field computation, trajectory simulation, and optical performance evaluation. Electrostatic field of lenses is evaluated via finite element method (FEM) with the core of COMSOL Multiphysics, while the trajectories and optical performance are computed under MATLAB environment. As are described in section 2, 3, and 4.

In the second part of this article, MPML2 system is introduced, and its preliminary lens system design is also presented. MPML2 system has been developed by the joint group in National Taiwan University. MPML2 is a multiple-source multiple-column system. Low energy (< 5keV) e-beams are arranged into a 100\*100 array to perform 22 nm direct-write exposure. In the 1<sup>st</sup> generation EOS design, beam blanker and deflector are eliminated. A three-electrode lens is used to focus the e-beam generated by the source. In section 5, the design concept of MPML2 is presented.

The preliminary lens design and simulation is shown in section 6.

## 2. Field Computation

Since it is the electric or magnetic field that changes the path of charged particles, field computation is the first step of electron optical analysis. Electrostatic potential ( $\Phi$ ) of the lens is determined by solving the Poisson equation

$$\nabla^2\Phi = -\rho/\epsilon \quad (1)$$

where  $\rho$  is the space charge density and  $\epsilon$  is the permittivity of the space. In practical use, the space charge density is so small that can be neglected to form the Laplace's equation

$$\nabla^2\Phi = 0 \quad (2)$$

However, the analytical solution of potential distribution merely exists even though the lens structure is quite simple. Thus, appropriate approximation or numerical techniques must be applied to solve the field distribution over the electron optical system.

COMSOL Multiphysics is one of the FEM solvers for plenty of engineering problems, and it is highly compatible with MATLAB. It provides a set of MATLAB command for geometrical parameter assign, simulation parameter setting, and computation result access. In our simulator, field computation process is done by solving Laplace's equation via COMSOL Multiphysics. Fig. 1 shows the mesh dividing result with COMSOL Multiphysics. Fig. 2 is the field computation result in 3-D with COMSOL Multiphysics.

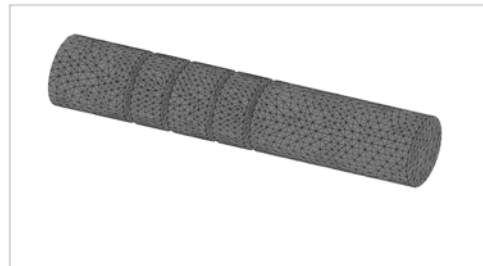


Fig. 1 A four-electrode lens structure after mesh dividing with COMSOL Multiphysics.

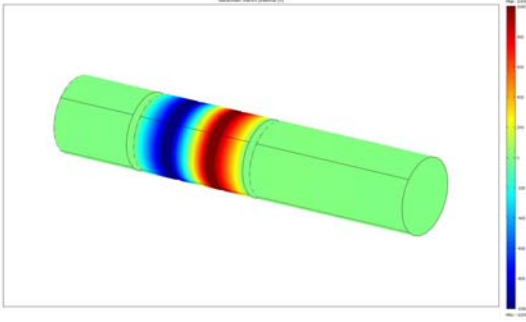


Fig. 2 The electric potential distribution of the four-electrode lens with COMSOL Multiphysics.

### 3. Trajectory Simulation

Electron trajectories reveal how the lens works, and there are two types of electron trajectories. One is the practical trajectory which is direct traced directly from the field distribution, and it is the real path of electron in the EOS. The other is the ideal trajectory, or Gaussian trajectory, which is computed under paraxial approximation and it, describes the perfect optical behavior. Gaussian trajectory is important to lens design and aberration evaluation.

#### 3.1 Practical Trajectory Simulation Result

Since individual beam in MPML2 is operated in low current and low energy. Interactions between electrons are neglect in this simulator. Hence the practical trajectory can be described by Lorentz's equation

$$\frac{d}{dt}(\gamma m_0 \bar{v}) = e\bar{E} \quad (3)$$

where  $m_0$  is rest mass of the electron,  $\bar{v}$  is the velocity  $e$  is electron charge,  $\bar{E}$  is electric field, and  $\gamma$  is the Lorentz factor in special relativity. To solve Lorentz's equation numerically and precisely, 4<sup>th</sup> order Runge-Kutta method is applied [6]. The concept of 4<sup>th</sup> order Runge-Kutta method is to evaluate the position and velocity of next step with a weighted sum of four new data predicted, and so that the discrete step error can be well controlled. Through the above-mentioned, real trajectory result can be obtained and simulated. Fig. 3 shows an example of three-electrode lens, in which the structure and simulation settings are listed in Table 1.

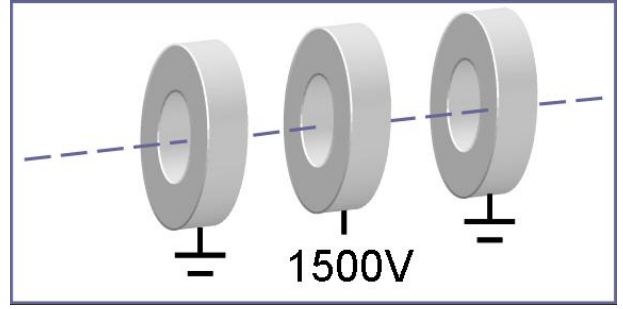


Fig. 3 An example of three-electrode lens with the 1500V applied to the middle electrode and ground at the other two electrodes.

Structure	Value
Electrode Length	50 $\mu m$
Gape Width	100 $\mu m$
Total Energy of Electron ( $E_0$ )	1keV

Table 1 Simulation settings of the three-electrode example.

Since above simulation settings and three-electrode structure defined have been determined, real trajectory is computed by direct interpolation method, and the result is plotted in Fig. 4 and Fig. 5.

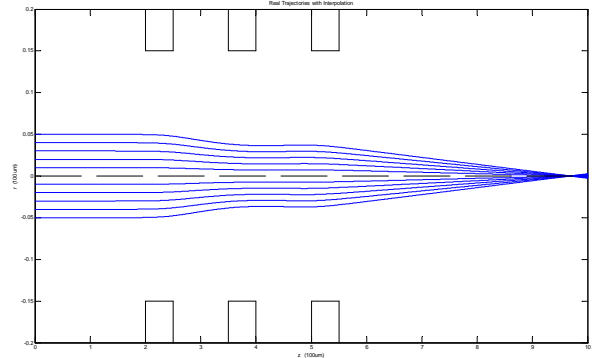


Fig. 4 Electron trajectories estimated with direct interpolation method.

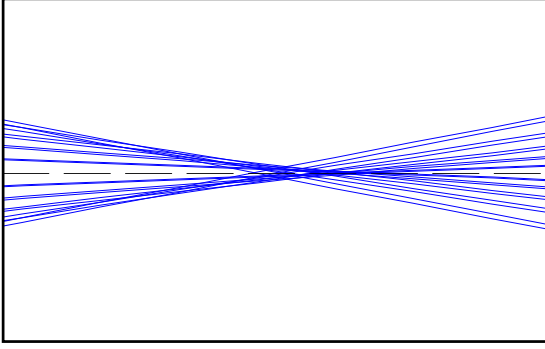


Fig. 5 Blur focus spot of real trajectories with direct interpolation method

### 3.2 Gaussian Trajectory Simulation Result

Gaussian trajectory equation is derived from Lorentz's equation and the assumption in which electrons travels close to the optical axis. Since ideal trajectories in static field would be time-invariant, Gaussian trajectory equation regards electron positions as a distribution in space and eliminates time in the equation [5]. In cylindrical coordinates  $(r, \theta, z)$ , it is represented as

$$r'' + \frac{\gamma\phi'}{2\hat{\phi}}r' + \frac{\gamma\phi''}{4\hat{\phi}}r = 0 \quad (4)$$

$\phi$  is the potential distribution on the axis and  $\hat{\phi}$  is a function of  $\phi$  and initial energy of electron. Both  $r$  and  $\phi$  are function of  $z$ , and prime ( $r'$ ) denotes derivative with respect to  $z$ . Since most of electrostatic lenses are rotational symmetrical, equation (4) is practical in electrostatic lens design. To solve equation (4) numerically, finite difference approximation is applied to the derivatives

$$\frac{dr(z)}{dz} = \frac{r(z+\Delta z) - r(z-\Delta z)}{2\Delta z} \quad (5)$$

$$\frac{d^2r(x)}{dz^2} = \frac{r(z+\Delta z) - 2r(z) + r(z-\Delta z)}{(\Delta z)^2} \quad (6)$$

where derivative is approximated by the slope of between the points before and back. Hence the Gaussian trajectory equation can be rearranging and represented as

$$r(z+\Delta z) = \frac{r(z) \cdot (8\hat{\phi} - \gamma\phi''\Delta z^2)}{(4\hat{\phi} + \gamma\phi'\Delta z)} + \frac{r(z-\Delta z) \cdot (\gamma\phi'\Delta z - 4\hat{\phi})}{(4\hat{\phi} + \gamma\phi'\Delta z)} \quad (7)$$

Thus, once the initial position and traveling direction are known, the whole path can be evaluated with equation (7). For the same cast in Table 1 and in Fig. 6, the corresponding focal point of the lens is founded with rays which are incident in parallel. Fig. 7 shows the zooming view at the focal point. It is clear that the Gaussian trajectory predicts the ideal optical property, since all the rays incident in parallel are focused to the same point, which is so-called image focal point.

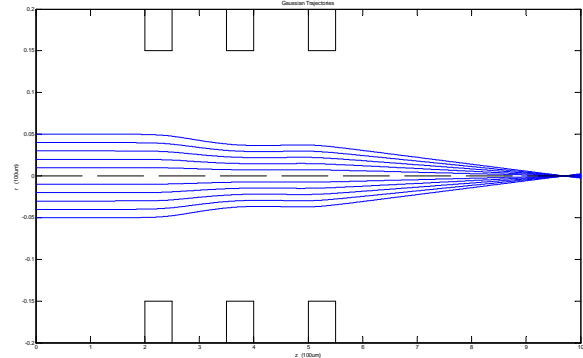


Fig. 6 Gaussian trajectories of 1keV electrons incident in parallel

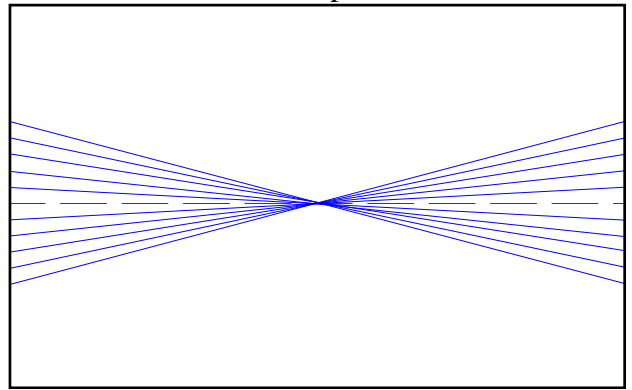


Fig. 7 The zooming view at the focal point

### 4. Optical Performance Evaluation

Since ideal and practical trajectories are computed, optical properties can be evaluated from them. The basic optical properties such as image plane, magnification, and focal points can be obtained from Gaussian trajectory. However, it is more significant to check image quality of the EOS designed. Aberrations are frequently used for image

quality analysis. Aberrations are the mismatches between the real image and the idea image estimated from Gaussian trajectory equation. They provide not only a standard manner to analyze blurring image, but a classification of causes of image degradation. Aberrations result from not only the geometrical design of the optical system, but the variation of initial energy of electrons. The former is called geometrical aberration, while the latter is called chromatic aberration [3] [5] [8].

The primary causes of image degradation are 3<sup>rd</sup> order geometrical aberrations and 3<sup>rd</sup> order chromatic aberration. 3<sup>rd</sup> order geometrical aberration is derived as

$$\begin{aligned} \Delta x_i = M \{ & C(x_o^2 + y_o^2) \cdot x_a + K(3x_o^2 x_o + y_o^2 x_o + 2x_o y_o y_o) \\ & + A(x_o^2 x_a - y_o^2 x_a + 2x_o y_o y_a) + F(x_o^2 + y_o^2) x_a \\ & + D(x_o^2 + y_o^2) x_o \} \end{aligned} \quad (8)$$

$$\begin{aligned} \Delta y_i = M \{ & C(x_o^2 + y_o^2) \cdot y_a + K(3y_o^2 y_o + x_o^2 y_o + 2y_o x_o x_o) \\ & + A(y_o^2 y_a - x_o^2 y_a + 2y_o x_o x_a) + F(x_o^2 + y_o^2) y_a \\ & + D(x_o^2 + y_o^2) x_o \} \end{aligned} \quad (9)$$

where the optical axis lies on z-axis. Suffix o, a, and i indicate object, aperture, and image plane.  $C$ ,  $K$ ,  $A$ ,  $F$  and  $D$  are the coefficients of spherical aberration, coma, astigmatism, field curvature, and distortion. 3<sup>rd</sup> order chromatic aberration is described as

$$\Delta x_i = -M(C_c x_o' + C_D x_o) \frac{\Delta \hat{\Phi}_o}{\hat{\Phi}_o} \quad (10)$$

where  $\Delta \hat{\Phi}_o$  represents the spread of initial energy of electrons.  $C_c$  is the central chromatic aberration coefficient, and  $C_D$  is the chromatic aberration coefficient of magnification. Details of derivation of aberration equations can be referred to reference [5] and reference [8].

Aberration analysis is useful in projection lithographic or microscopic systems. For probe-forming system, the spot size on wafer is more important than aberration coefficients. Thus direct ray tracing method rises and gains more and more interests. This method relies on computing a set of rays with different

initial conditions, and then analyzes the lens performance with the collective and statistic result of these rays. The more non-ideal effects the simulator can estimate, the more non-ideal factors are contains in the analysis results. Likewise, the more precise the ray trajectory is evaluated, the more accurate the analysis result obtained.

Here two methods for minimum spot size evaluation are proposed. First, as the green lines in Fig. 8 show, the spatial radius variation along optical axis is evaluated with its envelope of ray trajectories. Intuitively, the narrowest part of the envelope near the image plane is the

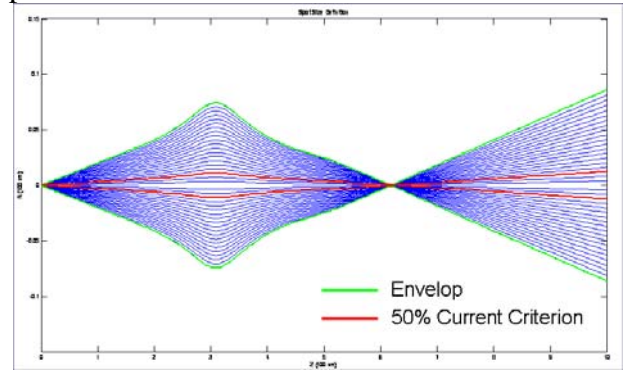


Fig. 8. Two methods for minimum spot size evaluation.

minimum spot requested in probe forming systems. This scheme treats each ray with the same weighting, so that each kind of initial conditions has the same significance to spot size. However, this treatment may not be consistent with the practice. Since there are always energy and current distributions inside the electron beam. To approach the reality, initial condition of rays should be considered. In e-beam lithographic system, since electron energy and charge density are two important parameters in resist exposure process, current distributions should be added into considerations during minimum spot size determination.

Special weightings are added to rays so that each ray is no longer an electron trajectory but a current flow. These weightings should follow the current distribution of the source. Thus, to apply this weighted simulation, the current distribution of the source should be known in advance. The red lines in Fig. 8 are

the envelope, which contains 50% beam current, and initial current distribution is assumed to be a normal distribution with respect to the emission angle. By means of this 50% envelope, minimum spot size can be determined with the consideration of current distribution.

### 5. MPML2 System Concept

Massively parallel maskless lithography (MPML2) is a next generation multiple electron beam system which is under development by an integrated research group of NTUEE, NTUME, and NSRRC. The objective of this project is to provide solution for 22nm-node semiconductor manufacturing with low-energy multiple e-beam direct-write technology. Fig. 9 is the schematic of the MPML2 system, which is a multiple-source multiple-column system arranged into 100\*100 arrays. Multiple-source structure releases the brightness requirement of electron emission element and avoids the current loss in beam splitting. Individual sources are designed to be controllable; hence beam current is adjustable. Neighboring beamlets are separated in 100  $\mu\text{m}$  so that the interaction and cross-talk can be reduced. The miniature electron optical elements are pure electrostatic, for the purpose to simplify the element shape and structure. Besides, each second electron detectors are placed near the wafer plane to capture the second electrons during exposure process. They provide feedback control loops to adjust the position drift and current variation of each beamlet. EOS of MPML2 is highly controllable to ensure exposure quality and uniformity.

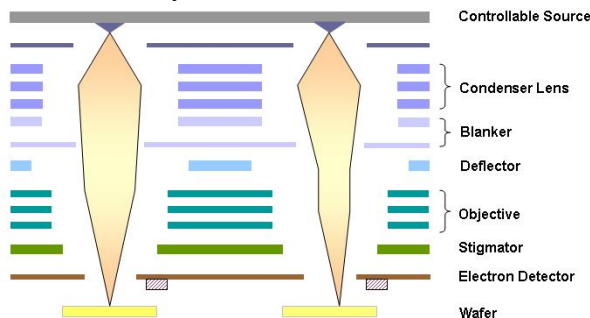


Fig. 9. Schematic of MPML2 system

### 6. Preliminary Lens Design

The preliminary electron optical system design of MPML2 is simplified into Fig. 10 and repeated into a 10\*10 array. This simplified system is utilized for test-bed of source, lens, and detector components design verification and performance evaluation. The blanker is replaced by controllable source to switch the beam on or off. The deflector is replaced by high resolution stage for 4" wafer, so that scanning of e-beams is achieved by stage motion.

In the preliminary system, cold field emission tips are used to generate electrons without heating the micro-columns. Since 1keV e-beam is desired, the emission tips are set to -1000V with respect to the ground of the whole system. The gate electrodes around the emission tips are driven to -900V to provide electric field around the tips to reduce the working function of field emission. A three-electrode einzel lens is laid with 1 mm away from the gate electrode, and the outer electrodes and wafer are set ground. So that the einzel lens makes no change of electron energy, and the electron energy is purely controlled by the accelerating voltage applied on the tips. Thus, parameters for the einzel lens are now reduced to three: central electrode voltage, electrode length, and spacer length. Fig. 11 is the side view of miniature einzel lenses. For the reason that the lens are built up with micro-fabrication processes, the shape of electrode are assume to be rectangular at the side and the length of electrodes or spacers are assume to be identical. Working distance is set to be ~3.25 mm, because the backscattering electron detector in this project is about 3 mm.

For the einzel lens, design of electrode and spacer dimensions begins from the considerations of process requirement. The material of electrodes is select in silicon, while the spacers are in Pyrex glass. Under the consideration of accessibility from local providers and bonding process, the preliminary thickness of electrodes is 250  $\mu\text{m}$ , and that of spacers is in 600  $\mu\text{m}$ . Thus, simulation starts from determination of the



central voltage. A roughly trail and error process is done at first to determined the range of voltages which enforces the beam converged and the minimum spot located near the 3.25 mm after the einzel lens. From Fig. 12, the central voltage is selected to be 2320V and the spot size at the 3.25 mm after einzel lens is evaluated in  $\sim 38\text{nm}$ .

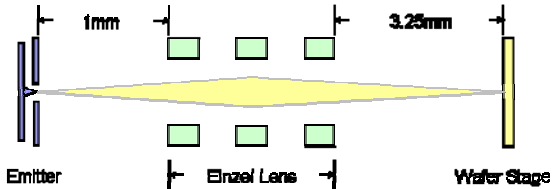


Fig. 10. Schematic of preliminary EOS design of MPML2

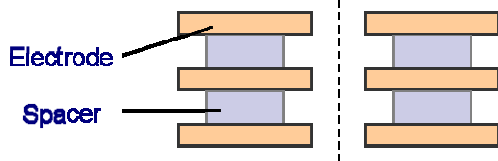


Fig. 11. Side view of einzel lens structure

Then we performed two simulations to clarify the effects of thickness variation of electrode or spacer. Fig. 13 shows the minimum spot size and location changes with the spacer thickness which varies within  $\pm 50\ \mu\text{m}$ . In the same manner, variation is added on electrode thickness, and the corresponding change of minimum spot size and location are plotted in Fig. 14. From the figures, we can find that the thickness variation of electrode and spacer has very little effect to minimum spot radius ( $< 2\ \text{nm}$ ).

In the previous design, the minimum spot radius is  $\sim 38\ \text{nm}$ , and it is too large for e-beam lithography. Thus, it is necessary to reduce minimum spot radius. However, in the preliminary system, there is only one lens to focus the beam, and hence, reduction of minimum spot radius can only be done by limiting the emission angle. Fig. 15 shows that minimum spot radius and position vary apparently with respect to emission angle. From Fig. 15, the emission

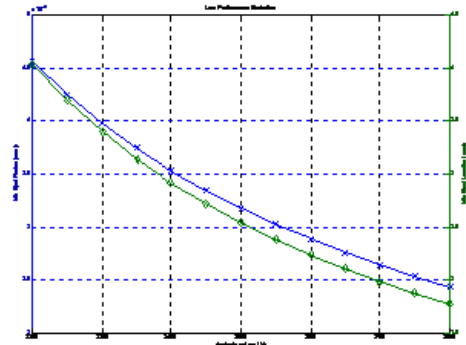


Fig. 12. Plot of minimum spot radius to central electrode voltage (in blue), and minimum spot position to central electrode voltage (in green)

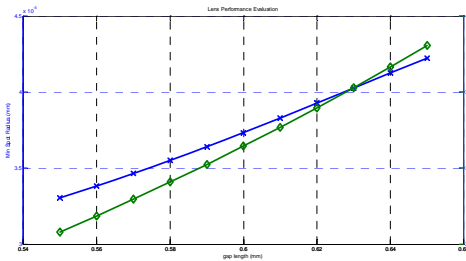


Fig. 13. Plot of minimum spot radius to spacer thickness (in blue), and minimum spot position to spacer thickness (in green)

angle should be reduced to 10 mrad for 10 nm beam radius, and 5 mrad for 1.2nm. Thus, beam limiting aperture can be applied at the region between source and lens. Fig. 16 shows the design parameters of the preliminary EOS of MPML2. The limiting aperture diameter is designed to be 3  $\mu\text{m}$  to achieve 1.2 nm beam radius. Hence, the preliminary EOS design of MPML2 has done with the assistance of the simulator.

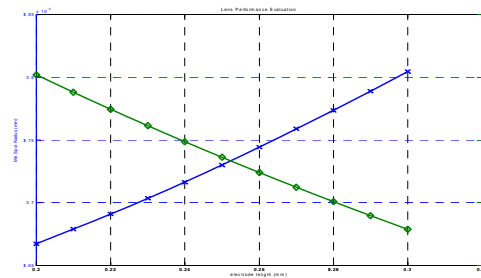


Fig. 14. Plot of minimum spot radius to electrode thickness (in blue), and minimum spot position to electrode thickness (in green)

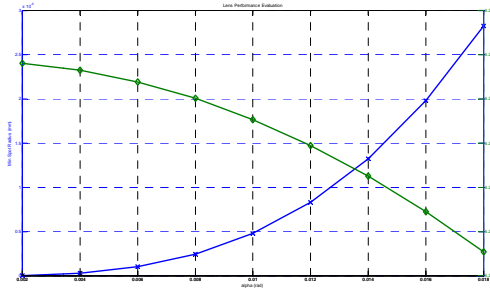


Fig. 15. Plot of minimum spot radius to emission angle (in blue), and minimum spot position to emission angle (in green)

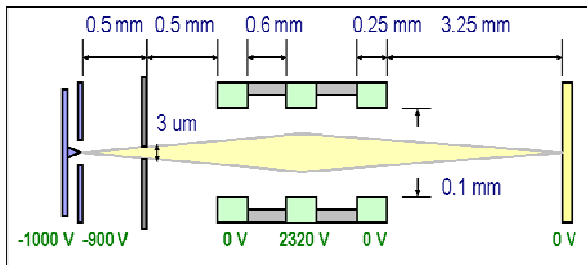


Fig. 16. Parameters of preliminary EOS for MPML2

## 7. Conclusion

Concept of MPML2 system is presented to be a highly controllable lithographic system for 22 nm node semiconductor manufacturing. For EOS design, a simulator is developed, and it is capable of trajectory computation and optical property evaluation in 2-D and 3-D environment. In addition, direct ray tracing method for minimum spot size is proposed and implemented. Finally Preliminary EOS design is completed with the simulator implemented.

## References

- [1] Bill Wilson, "Photolithography," *Connexions*, June 20, 2003, <http://cnx.org/content/m11367/1.1/>.
- [2] Burn J. Lin, "Immersion lithography and its impact on semiconductor manufacturing," *J. Microlith., Microfab., Microsyst.*, vol. 3, 2004.
- [3] Jon Orloff, *Handbook of charged particle optics*, CRC Press, 1997.
- [4] Matthew N. O. Sadiku, *Numerical Techniques in Electromagnetics second edition*, CRC Press, 2000.

[5] P. W. Hawkes and E.Kasper, *Principles of Electron Optics, Volume 1 Basic Geomtrical Optics*, Academic Press, 1996.

[6] Dennis G. Zill, Michael R. Cullen, *Differential Equations with Boundary-Value Problems fifth edition*, Brooks/Cole, 2000.

[7] DWO Heddle, *Electrostatic Lens Systems 1st Edition*, Adam Hilger, 1991.

[8] Ximen Hiye, *Aberration Theory in Electron and Ion Optics*, Academic Press, 1986.